nature immunology

E3 ubiquitin ligase RNF128 promotes innate antiviral immunity through K63-linked ubiquitination of TBK1

Guanhua Song[1,2], Bingyu Liu[1], Zhihui Li[2], Haifeng Wu[1], Peng Wang[1], Kai Zhao[1], Guosheng Jiang[2], Lei Zhang[1] & Chengjiang Gao[1]

TBK1 is essential for interferon-β (IFN-β) production and innate antiviral immunity. Here we identified the T cell anergy–related E3 ubiquitin ligase RNF128 as a positive regulator of TBK1 activation. RNF128 directly interacted with TBK1 through its protease-associated (PA) domain and catalyzed the K63-linked polyubiquitination of TBK1, which led to TBK1 activation, IRF3 activation and IFN-β production. Deficiency of RNF128 expression attenuated IRF3 activation, IFN-β production and innate antiviral immune responses to RNA and DNA viruses, *in vitro* and *in vivo*. Our study identified RNF128 as an E3 ligase for K63-linked ubiquitination and activation of TBK1 and delineated a previously unrecognized function for RNF128.

Innate immunity is the host's first line of defense against microbial invasion. Activation of the innate immune response requires pattern-recognition receptor (PRR) recognition of pathogen-associated molecular patterns (PAMPs)[1]. Viral nucleic acids, including DNA and RNA, are efficient PAMPs to initiate the innate antiviral immunity. PRRs that recognize these viral nucleic acids include TLR3 (ref. 2), RIG-I[3–5], MDA5 (ref. 6) and some DNA sensors such as cyclic GMP–AMP synthase (cGAS)[7]. Upon recognition of the nucleic acids, these PRRs recruit adaptors including TRIF, MAVS and STING to activate TBK1 (ref. 8). Activated TBK1 phosphorylates the transcription factors IRF3 and IRF7 to induce type I interferon expression[9]. Insufficient interferon production causes chronic infection, whereas excessive interferon production causes autoimmune and/or inflammatory disease. Thus, precise control of interferon production is critical for efficient viral clearance without harmful immunopathology.

Because the kinase TBK1 is crucial in the production of type I interferons, its activation must be tightly regulated to maintain immune homeostasis. TBK1 activation is regulated in a variety of ways, including protein ubiquitination and phosphorylation. The E3 ubiquitin ligases MIB1, MIB2 (ref. 10) and Nrdp1 (ref. 11) have been found to activate TBK1 by promoting its K63-linked polyubiquitination. However, MIB1, MIB2 and Nrdp1 mediate K63-linked polyubiquitination of TBK1 only in response to RNA virus and lipopolysaccharide (LPS), respectively[10,11]. The E3 ubiquitin ligase DTX4 (ref. 12) and TRAF-interacting protein (TRIP)[13] have been shown to negatively regulate TBK1 activation and antiviral response by promoting proteasomal degradation of TBK1, and the deubiquitinating enzymes CYLD[14] and USP2b[15] inhibit TBK1 activation by cleaving K63-linked ubiquitin chains from TBK1. Although these studies clearly demonstrate that these ligases and deubiquitinating enzymes are essential for TBK1 regulation, their roles have not been confirmed *in vivo*. Importantly, the E3 ubiquitin ligase responsible for K63-linked TBK1 polyubiquitination upon DNA-virus infection has not been identified.

RNF128 is a well-studied regulator involved in the induction and maintenance of T cell anergy[16–18]. However, the function of RNF128 in other immune responses is not known. Several other E3 ligases that regulate T cell anergy, such as Cbl-b, c-Cbl and Itch, have been demonstrated to have important roles in the regulation of innate immunity[19–21].

In the present study we demonstrated that T cell anergy–related E3 ubiquitin ligase RNF128 (also known as GRAIL) is an essential positive regulator of innate antiviral immunity to RNA virus and DNA virus. RNF128 knockdown or deficiency impaired IRF3 activation and IFN-β signaling. Consistently, *Rnf128*$^{-/-}$ mice were more susceptible than wild-type mice to infection with the RNA virus vesicular stomatitis virus (VSV) and the DNA virus herpes simplex virus type 1 (HSV-1). Mechanistically, RNF128 associated with TBK1 and promoted TBK1 kinase activity through conjugation of K63-linked ubiquitin chains. As such, our study identified RNF128 as a new E3 ligase for K63-linked ubiquitination of TBK1 to RNA and DNA viruses.

RESULTS

Virus infection induces RNF128 expression

We first measured RNF128 expression in mouse primary peritoneal macrophages and human monocytic leukemia (THP-1) cells stimulated with nucleic acid mimics poly(I:C) and interferon-stimulatory DNA (ISD). Expression of RNF128 mRNA and protein was higher in mouse peritoneal macrophages after stimulation with poly(I:C) and ISD than in unstimulated macrophages (**Fig. 1a** and **Supplementary Fig. 1a**). Expression of RNF128 mRNA and protein was also higher in THP-1 cells stimulated with poly(I:C) and ISD than in unstimulated

[1]Department of Immunology and Key Laboratory of Infection and Immunity of Shandong Province, Shandong University the School of Medicine, Jinan, China. [2]Institute of Basic Medicine, Shandong Academy of Medical Sciences, Jinan, China. Correspondence should be addressed to C.G. (cgao@sdu.edu.cn).

Received 27 July; accepted 21 September; published online 24 October 2016; doi:10.1038/ni.3588

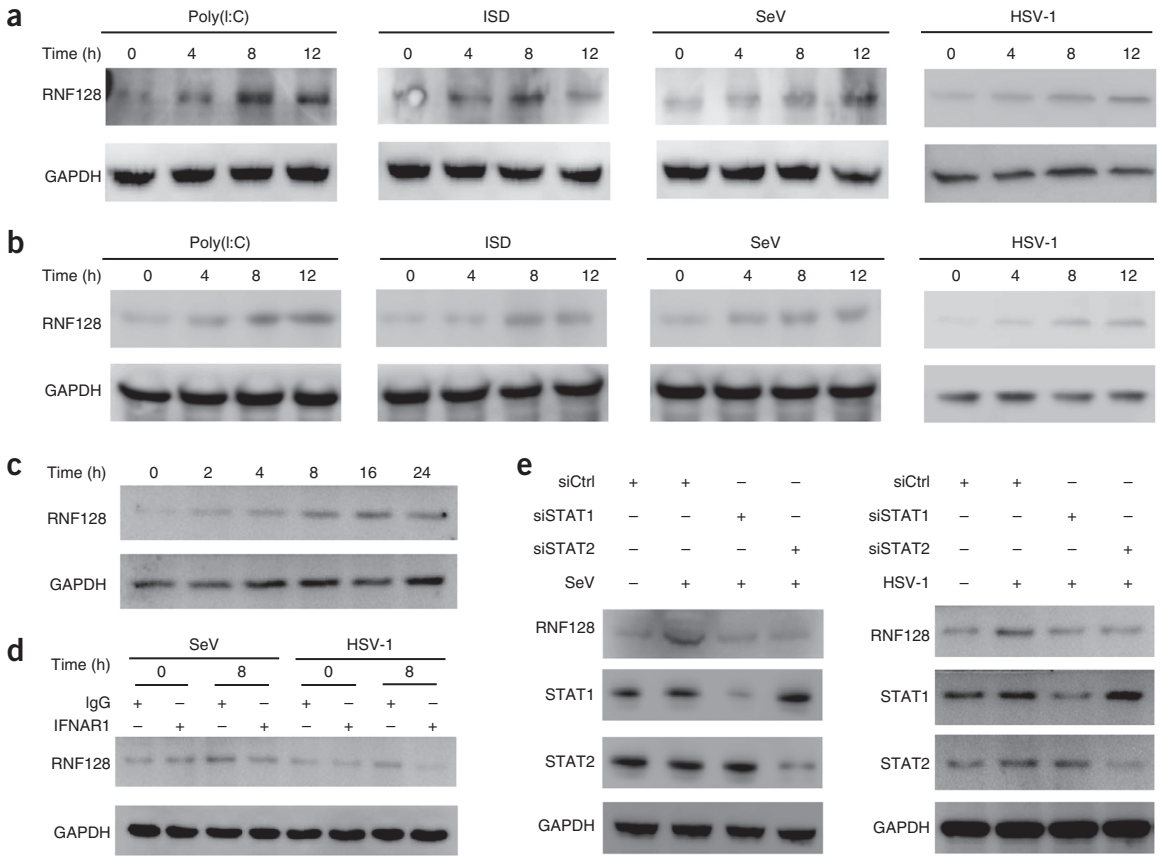

Figure 1 Viral infection induces RNF128 expression. (**a**,**b**) Immunoblot analysis of RNF128 protein expression in mouse peritoneal macrophages (**a**) and THP-1 cells (**b**) upon stimulation with poly(I:C) and ISD or infection with SeV and HSV-1 for 0, 4, 8 or 12 h. GAPDH was used as loading control. (**c**) Immunoblot analysis of RNF128 expression in mouse peritoneal macrophages treated with mouse recombinant IFN-β for 0, 2, 4, 8, 16 or 24 h. (**d**) Immunoblot analysis of RNF128 expression in mouse peritoneal macrophages pretreated with IFNAR1-specific antibody or control antibody (IgG) for 2 h then infected with SeV or HSV-1 for 8 h. (**e**) Immunoblot analysis of RNF128 expression in mouse peritoneal macrophages transfected with STAT1-specific siRNA (siSTAT1), siSTAT2 or control siRNA (siCtrl) for 48 h then infected with SeV or HSV-1 for 8 h. Data are representative of 3 independent experiments with similar results.

THP-1 cells (**Fig. 1b** and **Supplementary Fig. 1b**). Because poly(I:C) and ISD were considered mimics for double-stranded RNA and DNA, respectively[3,22], we further measured RNF128 expression after RNA- or DNA-virus infection. Infection with RNA virus Sendai virus (SeV) or HSV-1 increased expression of RNF128 mRNA and protein in mouse peritoneal macrophages and THP-1 cells, as compared to uninfected cells (**Fig. 1a**,**b** and **Supplementary Fig. 1a**,**b**).

Virus infection induces production of IFN-β, which binds to the IFN-β receptor and leads to the activation of STAT1 and STAT2 and transcription of interferon-stimulated genes[23]. IFN-β stimulation increased RNF128 protein expression in peritoneal macrophages (**Fig. 1c**). Furthermore, cells in which IFN-β signaling was blocked by an antibody to IFN-β receptor 1 (IFNRA1) showed attenuation of SeV- and HSV-1-induced RNF128 expression, compared to cells treated with a control antibody (**Fig. 1d**). Cells transfected with STAT1- and STAT2-specific small interfering RNA (siRNA) also showed attenuation of SeV- and HSV-1-induced RNF128 expression (**Fig. 1e**). Together, these data demonstrate that virus infection induces RNF128 expression, which indicates that RNF128 may have a role in antiviral innate immunity.

RNF128 positively regulates IRF3 activation and IFN-β production

To explore the function of RNF128 in the innate antiviral response, we designed three siRNAs specific for mouse RNF128 (mRNF128 siRNA1, siRNA2 or siRNA3) and transfected them into mouse primary peritoneal macrophages. Endogenous RNF128 mRNA and protein expression were attenuated after transfection with mRNF128 siRNA1 and mRNF128 siRNA2, whereas mRNF128 siRNA3 had only a minor effect (**Supplementary Fig. 2a**). Expression of *Ifnb1* (which encodes IFN-β) was decreased in peritoneal macrophages transfected with mRNF128 siRNA1 or mRNF128 siRNA2 upon simulation with poly(I:C) or ISD or infection with SeV or HSV-1, as compared to macrophages transfected with control siRNA (**Supplementary Fig. 2b**). Expression of *Il6* and *Tnf*, proinflammatory cytokines downstream of NF-κB signaling but not interferon signaling in peritoneal macrophages was not affected by mRNF128 siRNA1 or mRNF128 siRNA2 transfection (**Supplementary Fig. 2b**), but expression of *Cxcl10*, *Mx1* and *Ccl5*, which are induced downstream of IFN-β signaling, was decreased (**Supplementary Fig. 2b**). Notably, mRNF128 siRNA3, which had a negligible effect on *Rnf128* mRNA expression, did not attenuate expression of *Ifnb1*, *Cxcl10*, *Mx1* or *Ccl5* compared to control siRNA bearing a scrambled sequence (**Supplementary Fig. 2b**). Similarly, siRNA-mediated knockdown of human RNF128 expression in THP-1 cells also decreased poly(I:C)-, SeV-, ISD- and HSV-1-induced expression of *IFNB1*, *CXCL10*, *MX1* and *CCL5* mRNA but not the expression of *IL6* or *TNF* mRNA (**Supplementary Fig. 2c**,**d**), indicating the function of RNF128 in IFN-β signaling is conserved in mice and humans.

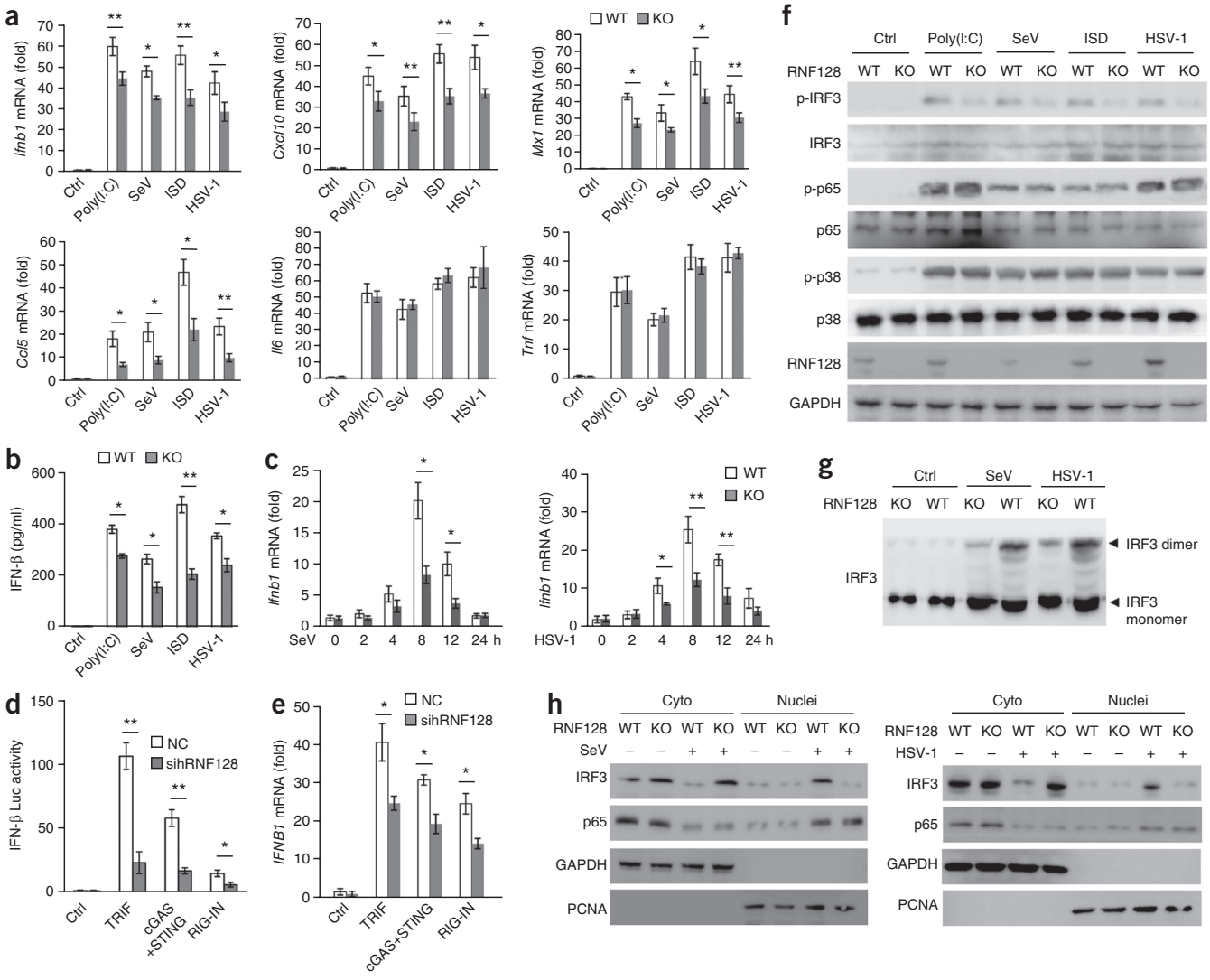

Figure 2 RNF128 positively regulates IFN-β signaling. (**a**) Expression of *Ifnb1*, *Cxcl10*, *Mx1*, *Ccl5*, *Il6* and *Tnf* mRNA in peritoneal macrophages from wild-type (WT) or *Rnf128*$^{-/-}$ (KO) mice stimulated with poly(I:C) or ISD or infected with SeV or HSV-1 for 8 h. Ctrl, control (no stimulation). (**b**) ELISA quantification of IFN-β secretion in WT or KO peritoneal macrophages treated as in **a**. (**c**) Time-course studies of *Ifnb1* expression in WT or KO peritoneal macrophages infected with SeV or HSV-1. (**d**) Luciferase (Luc) activity in HEK293 cells transfected with control siRNA (NC) or hRNF128 siRNA (sihRNF128) for 24 h and then transfected with IFN-β luciferase reporter together with expression plasmids for TRIF, cGAS+STING or RIG-IN for 24 h. Ctrl, empty vector. (**e**) *IFNB1* mRNA expression in HEK293 cells transfected with NC or sihRNF128 and then transfected with expression plasmids for TRIF, cGAS+STING or RIG-IN for 24 h. (**f**) Immunoblot analysis of phosphorylated (p-) IRF3, p65 and p38 in WT and KO peritoneal macrophages upon stimulation with poly(I:C) or ISD or infection with SeV or HSV-1. GAPDH served as loading control. Ctrl, no stimulation. (**g**) Immunoblot analysis of IRF3 dimerization with native PAGE in WT and KO peritoneal macrophages upon SeV or HSV-1 infection. (**h**) Immunoblot analysis of IRF3 and p65 protein in nuclear and cytoplasmic (cyto) fractions in WT and KO peritoneal macrophages infected with SeV or HSV-1. GAPDH served as cytoplasmic control. PCNA served as nuclear protein control. $^{*}P < 0.05$; $^{**}P < 0.01$ (two-tailed Student's *t*-test). Data are from 3 independent experiments (mean ± s.d. of triplicate assays (**a**,**b**–**d**,**e**)) or are representative of 3 independent experiments with similar results (**f**–**h**).

To confirm the function of RNF128 in IFN-β signaling, we prepared primary peritoneal macrophages from *Rnf128*$^{-/-}$ mice and wild-type littermates. Compared to macrophages from wild-type mice, macrophages from *Rnf128*$^{-/-}$ mice showed lower IFN-β expression (**Fig. 2a**) and secretion (**Fig. 2b**) after stimulation with poly(I:C) or ISD or infection with SeV or HSV-1. Expression of *Cxcl10*, *Mx1* and *Ccl5* mRNA was also decreased (**Fig. 2a**). Expression of *Il6* and *Tnf* mRNA was not impaired in *Rnf128*$^{-/-}$ macrophages in these conditions (**Fig. 2a**). Time-course studies showed that SeV- or HSV-1-induced *Ifnb1* expression was detected as early as 4 h after infection and peaked at 8 h after infection in wild-type mice, whereas the expression of *Ifnb1* mRNA in *Rnf128*$^{-/-}$ macrophages was greatly decreased at these time points (**Fig. 2c**). LPS-induced expression of *Ifnb1*, *Cxcl10*, *Mx1* and *Ccl5*, but not *Il6* and *Tnf*, was also impaired in *Rnf128*$^{-/-}$ macrophages, as compared to wild-type macrophages (**Supplementary Fig. 2e**).

Transfection of HEK293 cells with TRIF, cGAS and STING mixed in equal amounts (cGAS+STING) or two N-terminal caspase-associated and recruitment domains of RIG-I (RIG-IN) induced IFN-β promoter–driven luciferase activity (**Fig. 2d**) and *IFNB1* mRNA expression (**Fig. 2e**), and siRNA-mediated knockdown of RNF128 expression attenuated these effects (**Fig. 2d**,**e**). In contrast, ectopic expression of RNF128 in HEK293 cells markedly increased TRIF-, RIG-IN- and cGAS+STING-induced IFN-β promoter–driven

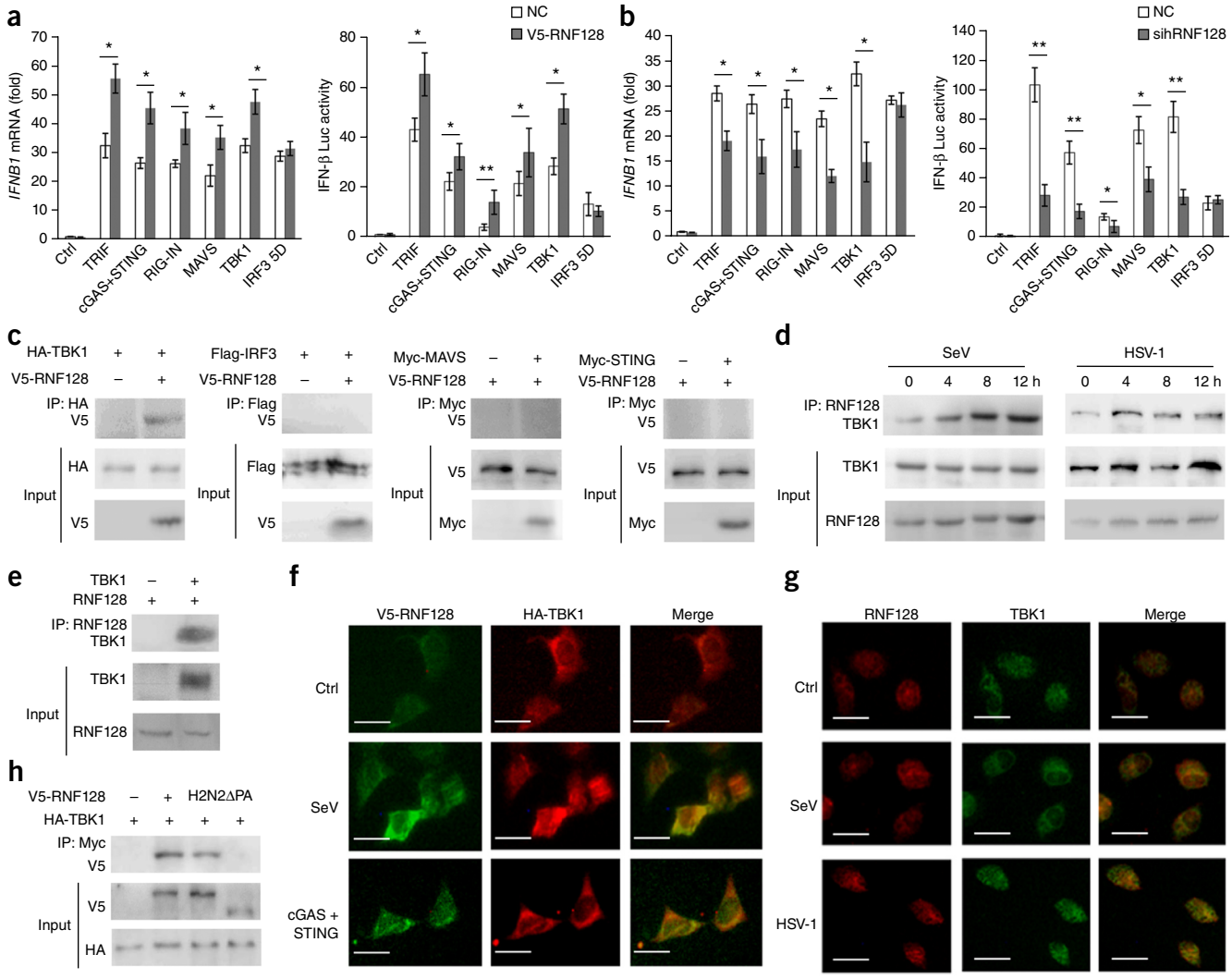

Figure 3 RNF128 targets TBK1. (**a**) Expression of *IFNB1* mRNA and luciferase (Luc) activity of IFN-β promoter reporter in HEK293 cells transfected with expression plasmids for TRIF, cGAS+STING, RIG-IN, MAVS, TBK1 or IRF3 5D along with V5-RNF128 or control vector (NC) for 24 h. Ctrl, control (empty vector). (**b**) Expression of *Ifnb1* mRNA and luciferase activity of IFN-β promoter reporter in HEK293 cells transfected with control siRNA (NC) or hRNF128 siRNA (sihRNF128) for 24 h and then transfected with expression plasmids for TRIF, cGAS+STING, RIG-IN, MAVS, TBK1 or IRF3 5D along with RNF128 expression plasmid for 24 h. (**c**) Immunoprecipitation and immunoblot analysis of V5-RNF128-WT with Flag-IRF3, Myc-MAVS, Myc-STING or HA-TBK1 in HEK293 cells. IP, immunoprecipitation. (**d**) Immunoprecipitation and immunoblot analysis of RNF128 and TBK1 in mouse peritoneal macrophages infected with SeV or HSV-1 for various times. (**e**) *In vitro* interaction analysis of RNF128 with TBK1 using *in vitro*–translated RNF128 and TBK1. (**f**) V5- and HA-specific immunostaining of HEK293 cells transfected with V5-RNF128-WT, HA-TBK1 and expression plasmid for cGAS+STING or transfected with V5-RNF128-WT and HA-TBK1 then infected with SeV for 8 h. Scale bars, 10 μm. (**g**) Immunostaining of primary peritoneal macrophages infected with SeV or HSV-1 for 8 h then immunostained with anti-TBK1 and anti-RNF128. Scale bars, 10 μm. (**h**) Immunoprecipitation and immunoblot analysis of V5-RNF128-WT, V5-RNF128-H2N2 or V5-RNF128-ΔPA with HA-TBK1 in HEK293 cells. $*P < 0.05$, $**P < 0.01$ (two-tailed Student's *t*-test). Data are from 3 independent experiments (**a**,**b**; mean ± s.d. of triplicate assays) or are representative of 3 independent experiments with similar results (**c**–**h**).

luciferase activity and *IFNB1* mRNA expression (**Supplementary Fig. 2f**,**g**). Together, these data demonstrate that RNF128 positively regulates IFN-β production downstream of TLR3-, RIG-I- and cGAS-mediated pathways.

IFNB1 transcription requires binding of the transcription factors IRF3, NF-κB and AP-1 to its promoter enhancer region[24]. NF-κB and AP-1 bind to positive regulatory domains (PRDs) II and IV, respectively, and IRF3 binds to the overlapping PRDs I and III. RNF128 overexpression increased TRIF-, MAVS- and cGAS+STING-induced activation of IFN-β promoter reporter in HEK293 cells, compared to control vector (**Supplementary Fig. 3a**). RNF128 also increased the activation of the reporter containing IFN-β promoter PRDs I–III (**Supplementary Fig. 3a**). By contrast, we did not observe an appreciable difference between the RNF128 expression plasmid and the control vector in activation of reporters containing IFN-β promoter PRD II and PRD IV (**Supplementary Fig. 3a**). These data suggest that RNF128 regulates IFN-β production mainly through the activation of IRF3.

IRF3 activation requires phosphorylation on multiple sites at the C-terminal end of IRF3 (ref. 25). Overexpression of RNF128 increased TRIF-, MAVS- and STING+cGAS-induced IRF3 phosphorylation (**Supplementary Fig. 3b**). Notably, MAVS-induced IRF3 phosphorylation was increased by RNF128 overexpression in a dose-dependent manner (**Supplementary Fig. 3c**). To further confirm that RNF128 facilitates IRF3 activation, we compared IRF3 activation in

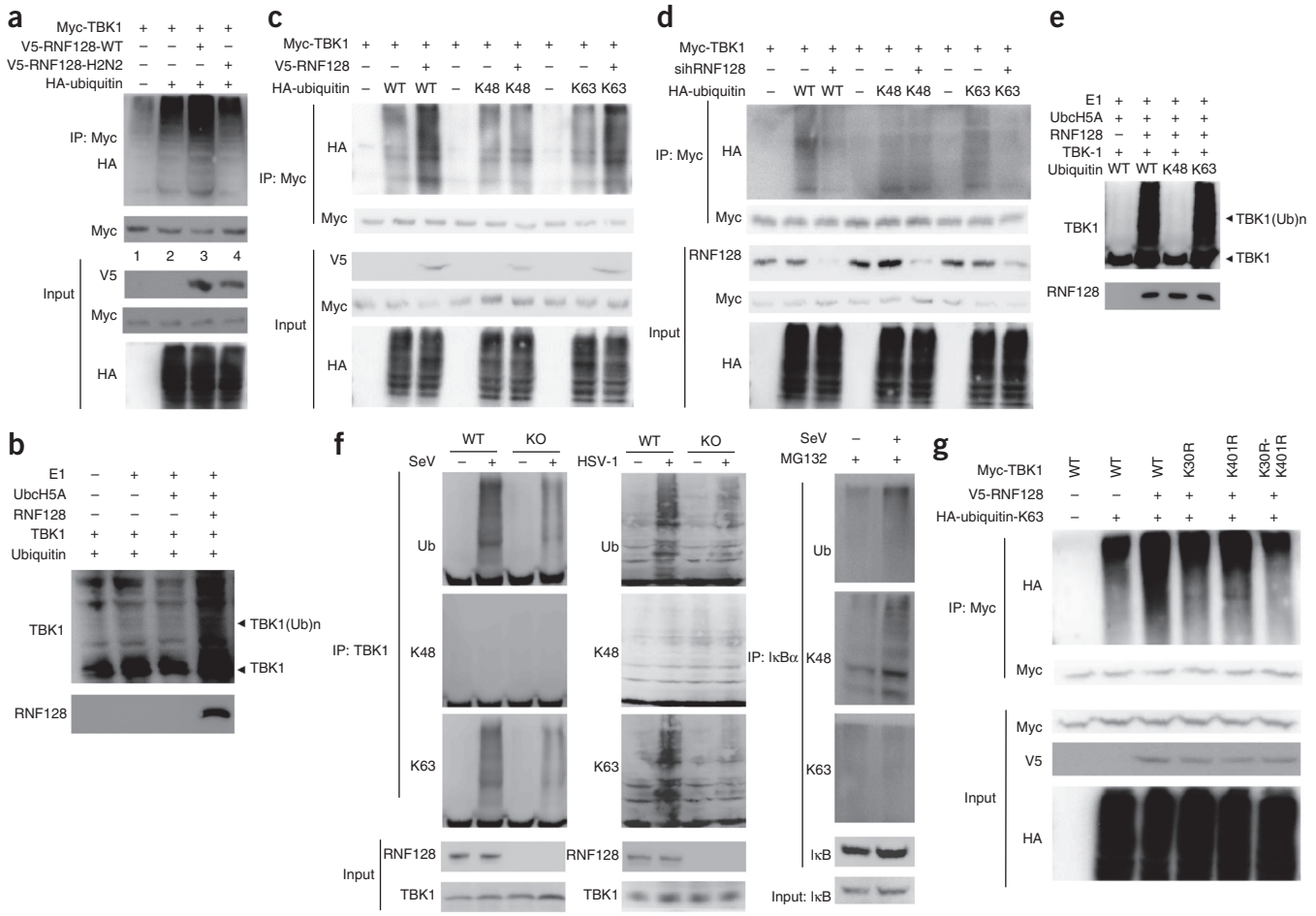

Figure 4 RNF128 promotes K63-linked ubiquitination of TBK1. (**a**) Coimmunoprecipitation analysis of TBK1 ubiquitination in HEK293 cells transfected with Myc-TBK1-WT or HA-ubiquitin-WT in the presence of control vector, V5-RNF128-WT or V5-RNF128-H2N2 expression plasmid. IP, immunoprecipitation. (**b**) *In vitro* TBK1 ubiquitination assay using *in vitro*–translated RNF128 and TBK1 in the presence of ubiquitin, E1 or E2 (UbcH5A). (**c**) Coimmunoprecipitation analysis of TBK1 ubiquitination in HEK293 cotransfected with Myc-TBK1-WT, V5-RNF128-WT or control vector and HA-ubiquitin-WT, HA-ubiquitin-K48 or HA-ubiqutin-K63 plasmids. (**d**) Coimmunoprecipitation analysis of TBK1 ubiquitination in HEK293 cells transfected with control siRNA or hRNF128 siRNA (sihRNF128) for 24 h then transfected with HA-ubiquitin-WT, HA-ubiquitin-K48 or HA-ubiquitin-K63 expression plasmids together with Myc-TBK1-WT. (**e**) *In vitro* TBK1 ubiquitination (TBK1(Ub)n) assay using *in vitro*–translated RNF128 and TBK1 in the presence of ubiquitin-WT, ubiquitin-K63 or ubiquitin-K48 with E1 and UbCH5A. (**f**) Coimmunoprecipitation analysis of TBK1 ubiquitination in primary macrophages from WT and *Rnf128*$^{-/-}$ (KO) mice infected with SeV or HSV-1. IκBα ubiquitination in primary macrophages infected with SeV were used as control. (**g**) Coimmunoprecipitation analysis of TBK1 ubiquitination in HEK293 cells cotransfected with expression plasmids for Myc-TBK1-WT or Myc-TBK1-K30R, Myc-TBK1-K401R or Myc-TBK1-K30R-K401R along with V5-RNF128 and/or HA-ubiquitin-K63 plasmids. Data are representative of 3 independent experiments with similar results.

primary peritoneal macrophages from *Rnf128*$^{-/-}$ and wild-type mice. Poly(I:C)-, SeV-, ISD- and HSV-1-induced IRF3 phosphorylation was lower in *Rnf128*$^{-/-}$ macrophages (**Fig. 2f**). In contrast, phosphorylation of p65 and p38 was not impaired in *Rnf128*$^{-/-}$ macrophages after infection (**Fig. 2f**). IRF3 forms a homodimer and then moves into the nucleus[26]. Consistent with decreased IRF3 phosphorylation, IRF3 dimerization (**Fig. 2g**) and nuclear translocation (**Fig. 2h**) were lower in *Rnf128*$^{-/-}$ macrophages infected with SeV or HSV-1 than in wild-type macrophages, whereas SeV- and HSV-1-induced nuclear translocation of p65 were not affected in *Rnf128*$^{-/-}$ cells (**Fig. 2h**). Taken together, these data demonstrate that RNF128 positively regulates IRF3 activation to regulate IFN-β production.

RNF128 targets TBK1

We next sought to determine the molecular mechanisms by which RNF128 enhances type I interferon signaling. Transfection of an RNF128 expression plasmid further increased TRIF-, cGAS+STING-, RIG-IN-, MAVS- and TBK1-induced *IFNB1* expression compared to transfection of control vector in HEK293 cells (**Fig. 3a**), whereas *IFNB1* expression induced by an IRF3 variant in which S396, S398, S402, S404 and S405 were replaced by the phosphomimetic aspartate (IRF3 5D) was not enhanced by RNF128 overexpression (**Fig. 3a**). Similarly, TRIF-, cGAS+STING-, RIG-IN-, MAVS- and TBK1-induced *IFNB1* promoter activity was increased in HEK293 cells transfected with an RNF128 expression plasmid, whereas IRF3 5D–induced *IFNB1* promoter activity was not (**Fig. 3a**). Transfection of human RNF128 (hRNF128) siRNA3 into HEK293 cells substantially attenuated TRIF-, cGAS+STING-, RIG-IN-, MAVS- and TBK1-induced *IFNB1* mRNA expression and promoter activation, whereas IRF3 5D–induced *IFNB1* mRNA expression and promoter activation were not impaired by hRNF128 siRNA3 (**Fig. 3b**). These data suggested that RNF128 may enhance type I interferon signaling by targeting TBK1.

To confirm that RNF128 targets TBK1, we investigated the interaction between RNF128 and TBK1. When cotransfected into HEK293

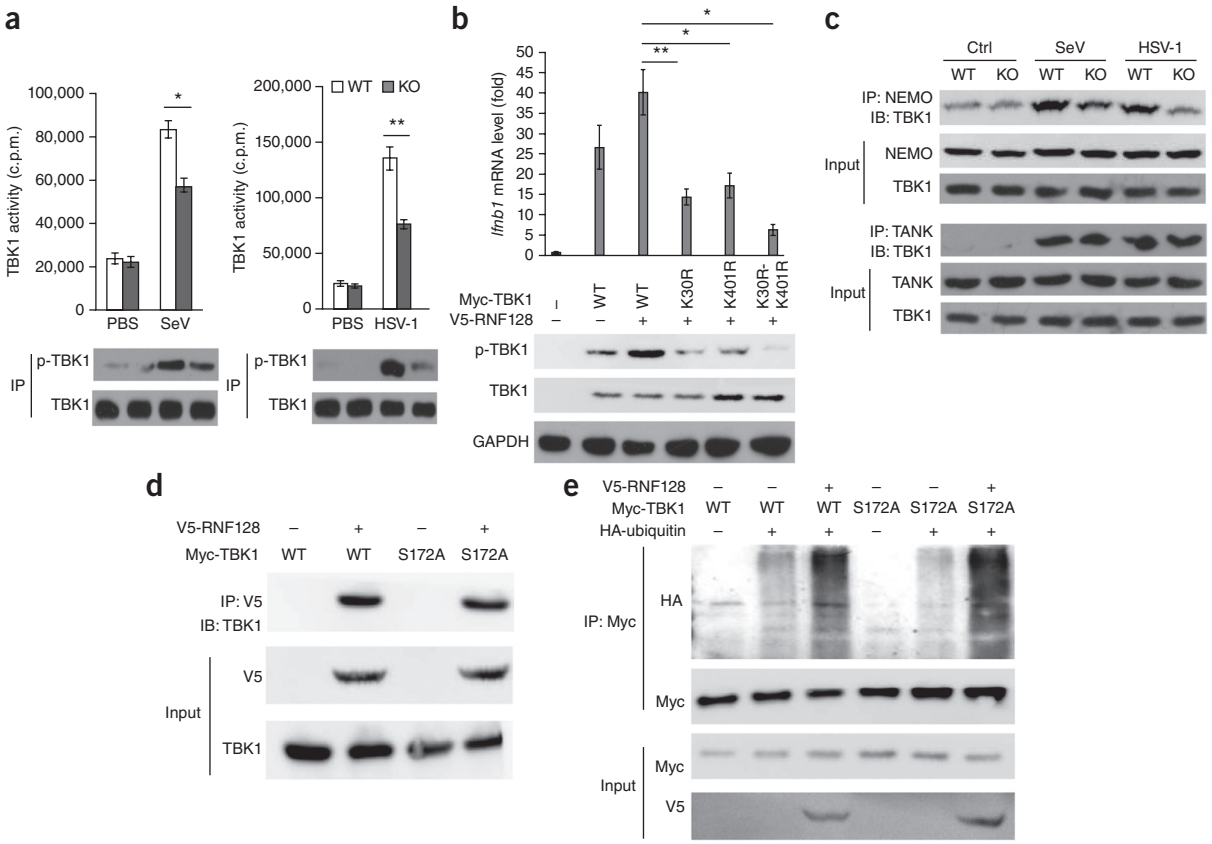

Figure 5 RNF128 promotes TBK1 activation. (**a**) TBK1 kinase activity in WT or *Rnf128*$^{-/-}$ (KO) mouse peritoneal macrophages infected with SeV or HSV-1 for 6 h (top). Immunoblot analysis of TBK1 and phosphorylated (p-) TBK1 in the TBK1 immunoprecipitates (bottom). IP, immunoprecipitation. (**b**) qRT-PCR analysis of *Ifnb1* mRNA expression (top) and immunoblot analysis of p-TBK1 (bottom) in *Tbk1*$^{-/-}$ MEFs transfected with Myc-TBK1-WT, Myc-TBK1-K30R, Myc-TBK1-K401R or Myc-TBK1-K30R-K401R and V5-RNF128-WT expression plasmids. (**c**) Coimmunoprecipitation analysis of NEMO or TANK with TBK1 in WT and *Rnf128*$^{-/-}$ (KO) peritoneal macrophages infected with SeV or HSV-1 for 8 h. (**d**) Coimmunoprecipitation analysis of V5-RNF128-WT with Myc-TBK1-WT or Myc-TBK1-S172A plasmids transfected into HEK293 cells. (**e**) Coimmunoprecipitation analysis of TBK1 ubiquitination in HEK293 cells transfected with V5-RNF128-WT and HA-ubiquitin-WT in the presence of control vector, Myc-TBK1-WT or Myc-TBK1-S172A expression plasmid. $^{*}P < 0.05$, $^{**}P < 0.01$ (two-tailed Student's *t*-test). Data are from 3 independent experiments (**a**,**b**; mean ± s.d. of triplicate assays) or are representative of 3 independent experiments with similar results (**a**–**e**).

cells, V5-tagged RNF128 (V5-RNF128) coimmunoprecipitated with HA-tagged TBK1 (HA-TBK1) (**Fig. 3c**). However, V5-RNF128 did not coimmunoprecipitate with Flag-tagged IRF3 (Flag-IRF3), Myc-tagged MAVS (Myc-MAVS) or Myc-STING when overexpressed in HEK293 cells (**Fig. 3c**). Endogenous RNF128 and TBK1 coimmunoprecipitated in mouse peritoneal macrophages (**Fig. 3d**), suggesting a constitutive interaction between the two proteins. Notably, the interaction between endogenous RNF128 and TBK1 was enhanced upon SeV or HSV-1 infection (**Fig. 3d**). An interaction between endogenous RNF128 and TBK1 was also detected in THP-1 cells (**Supplementary Fig. 4a**). In addition, a mixture of RNF128 and TBK1 generated in an *in vitro* protein expression system coimmunoprecipitated in pull-down assays with anti-RNF128 (**Fig. 3e**), indicating a direct interaction between RNF128 and TBK1.

Immunostaining with V5- and HA-specific antibodies showed a very low degree of colocalization between V5-RNF128 and HA-TBK1 transfected into HEK293 cells (**Fig. 3f**). Infection of SeV or ectopic expression of cGAS+STING increased colocalization between V5-RNF128 and HA-TBK1 (**Fig. 3f**). Similarly, we detected a low degree of colocalization between endogenous RNF128 and TBK1 in mouse peritoneal macrophages (**Fig. 3g**), but colocalization was greatly enhanced after infection with SeV or HSV-1 (**Fig. 3g**).

The PA domain of RNF128 captures target proteins for cytosolic ubiquitination, and the RING finger domain facilitates the ubiquitination of captured substrates[27]. To define the domains of RNF128 that bound to TBK1, we cotransfected HEK293 cells with HA-TBK1 and either wild-type V5-RNF128 (V5-RNF128-WT) or one of two RNF128 mutants—V5-RNF128-H2N2, which contains point mutations in the RING domain, or V5-RNF128-ΔPA, which lacks the PA domain. HA-TBK1 coimmunoprecipitated with V5-RNF128-WT and V5-RNF128-H2N2, but not with V5-RNF128-ΔPA (**Fig. 3h**), indicating that the PA domain is necessary for RNF128–TBK1 association. Consistently, V5-RNF128-ΔPA did not increase TRIF-, MAVS- or cGAS+STING-induced interferon-stimulated response element (ISRE) promoter activation or IRF3 phosphorylation in HEK293 cells compared to V5-RNF128-WT (**Supplementary Fig. 4b,c**). Overall, these results demonstrate that RNF128 targets and physically interacts with TBK1 through the PA domain of RNF128.

RNF128 promotes K63-linked ubiquitination of TBK1

RNF128 is a RING-type E3 ubiquitin ligase that has been reported to promote the ubiquitination of several substrates[18,27–29]. To investigate whether the E3 ligase activity of RNF128 was involved in the regulation of TBK1 activation, we transfected Myc-TBK1 into HEK293

cells together with the V5-RNF128 constructs described above. Coimmunoprecipitation experiments showed that TBK1 ubiquitination was markedly increased in the presence of RNF128 expression plasmid (**Fig. 4a**). Notably, V5-RNF128-H2N2 did not increase TBK1 polyubiquitination (**Fig. 4a**). Consistently, V5-RNF128-H2N2 did not increase TRIF-, MAVS- or cGAS+STING-induced ISRE promoter activation or IRF3 phosphorylation in HEK293 cells, as compared to V5-RNF128-WT (**Supplementary Fig. 4b**). RNF128 directly ubiquitinated TBK1 in *in vitro* ubiquitination assays in the presence of E1 activating enzymes and E2 conjugating enzymes (**Fig. 4b**).

To further investigate RNF128-mediated TBK1 polyubiquitination, we used mutants in which all lysine residues except K48 or K63 were replaced with arginine (HA-ubiquitin-K48 and HA-ubiquitin-K63). RNF128-mediated polyubiquitination of TBK1 was significantly increased in the presence of wild-type HA-ubiquitin (HA-ubiquitin-WT) or HA-ubiquitin-K63 but not HA-ubiquitin-K48 (**Fig. 4c**). In addition, siRNA-mediated knockdown of RNF128 expression substantially attenuated TBK1 ubiquitination in HEK293 cells transfected with HA-ubiquitin-WT or HA-ubiquitin-K63 but not HA-ubiquitin-K48 (**Fig. 4d**). *In vitro* ubiquitination assays with recombinant ubiquitin-WT, ubiquitin-K48 and ubiquitin-K63 showed that TBK1 ubiquitination was induced in the presence of E1, E3 and RNF128 together with ubiquitin-WT or ubiquitin-K63 but not ubiquitin-K48 (**Fig. 4e**). These data indicate that RNF128 mediates K63-linked ubiquitination of TBK1.

Next, we measured TBK1 ubiquitination in *Rnf128*$^{-/-}$ and wild-type primary macrophages after SeV or HSV-1 infection. We observed an increase in K63-linked TBK1 ubiquitination in wild-type macrophages, but not in *Rnf128*$^{-/-}$ macrophages, after SeV or HSV-1 infection (**Fig. 4f**). In contrast, SeV-induced MAVS ubiquitination and HSV-1-induced STING ubiquitination were not impaired in *Rnf128*$^{-/-}$ macrophages (**Supplementary Fig. 4d,e**). As a control, we examined the effects of SeV infection and found that it greatly increased K48-linked but not K63-linked polyubiquitination of the inhibitory cytoplasmic NF-κB chaperone IκBα (**Fig. 4f**), confirming the validity of the K48- and K63-specific antibodies.

Structural studies have shown that K63-linked polyubiquitination of TBK1 at K30 and K401 is required for its catalytic activation[30]. To investigate whether RNF128 promotes TBK1 ubiquitination through K30 or K401, we constructed Myc-TBK1 variants with point mutations K30R, K401R or both (Myc-TBK1-K30R, Myc-TBK1-K401R or Myc-TBK1-K30R-K401R, respectively) and transfected them into HEK293 cells together with V5-RNF128-WT. Myc-TBK1-K30R, Myc-TBK1-K401R and Myc-TBK1-K30R-K401R showed low TBK1 ubiquitination induced by V5-RNF128-WT (**Fig. 4g**). Taken together, these data demonstrate that RNF128 promotes K63-linked ubiquitination of TBK1 at K30 and K401.

RNF128 promotes TBK1 activation

To determine whether RNF128-induced TBK1 ubiquitination affects TBK1 activation, we immunoprecipitated TBK1 from mouse peritoneal macrophages and performed *in vitro* TBK1 kinase assays. TBK1 kinase activity was increased in wild-type macrophages upon SeV or HSV-1 infection (**Fig. 5a**), whereas SeV- and HSV-1-induced TBK1 kinase activity was greatly decreased in *Rnf128*$^{-/-}$ macrophages (**Fig. 5a**). SeV- and HSV-1-induced TBK1 phosphorylation was also decreased in *Rnf128*$^{-/-}$ macrophages (**Fig. 5a**). Furthermore, overexpression of RNF128 increased TBK1 kinase activity after SeV infection in HEK293 cells (**Supplementary Fig. 5a**), and siRNA-mediated knockdown of RNF128 expression in peritoneal macrophages attenuated TBK1 kinase activity after SeV infection (**Supplementary Fig. 5b**).

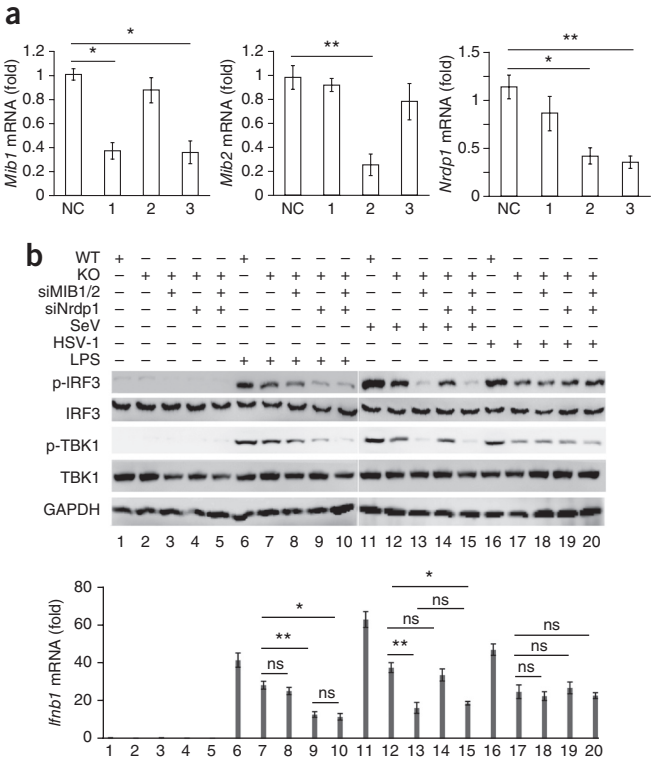

Figure 6 RNF128 is a general regulator of TBK1 activation. (**a**) qRT-PCR analysis of *Mib1*, *Mib2* and *Nrdp1* mRNA expression in mouse peritoneal macrophages transfected with control siRNA (NC) or targeted siRNA1–siRNA3 (1–3) for 48 h. (**b**) qRT-PCR analysis of *Ifnb1* mRNA expression (bottom) and immunoblot analysis of phosphorylated (p-) IRF3 and p-TBK1 (top) in *Rnf128*$^{-/-}$ (KO) peritoneal macrophages transfected with Mib1-1, Mib1-3 and Mib2-2 mixed at equal ratio (siMIB1/2) and/or a mixture of siNrdp1-2 and siNrdp1-3 (siNrdp1) and stimulated with LPS or infected with SeV or HSV-1. Peritoneal macrophages from wild-type (WT) mice were used controls. $^{*}P < 0.05$; $^{**}P < 0.01$; ns, not significant (two-tailed Student's *t*-test). Data are from 3 independent experiments (**a**,**b**; mean ± s.d. of triplicate assays) or are representative of 3 independent experiments with similar results (**b**).

Next, Myc-TBK1-WT, Myc-TBK1-K30R, Myc-TBK1-K401R and Myc-TBK1-K30R-K401R were transfected into *Tbk1*$^{-/-}$ mouse embryonic fibroblasts (MEFs). Myc-TBK1-WT restored TBK1 activation in *Tbk1*$^{-/-}$ MEFs, as assessed by TBK1 phosphorylation and *Ifnb1* expression (**Fig. 5b**), and transfection of the RNF128 expression plasmid further increased TBK1 phosphorylation and TBK1-induced *Ifnb1* expression in *Tbk1*$^{-/-}$ MEFs (**Fig. 5b**). However, phosphorylation of TBK1-K30R, TBK1-K401R and TBK1-K30R-K401R and expression of *Ifnb1* were greatly decreased in the presence of RNF128 in *Tbk1*$^{-/-}$ MEFs (**Fig. 5b**).

How K63-linked ubiquitination of TBK1 leads to TBK1 phosphorylation is not clear. In one model, K63-ubiquitinated TBK1 recruits adaptors such as NEMO and TANK to trigger higher-order oligomerization of TBK1–adaptor complexes, resulting in *trans*-autophosphorylation and activation of TBK1 (ref. 31). Consistent with this model, binding of NEMO to TBK1 was lower in *Rnf128*$^{-/-}$ peritoneal macrophages than in wild-type macrophages after SeV or HSV-1 infection (**Fig. 5c**). Binding of TANK to TBK1 was not impaired in *Rnf128*$^{-/-}$ peritoneal macrophages (**Fig. 5c**).

After activation, TBK1 was phosphorylated at a single serine residue, S172, which is required for TBK1 kinase activity[32]. Indeed, we found that Myc-TBK1 with a S172A substitution (Myc-TBK1-S172A)

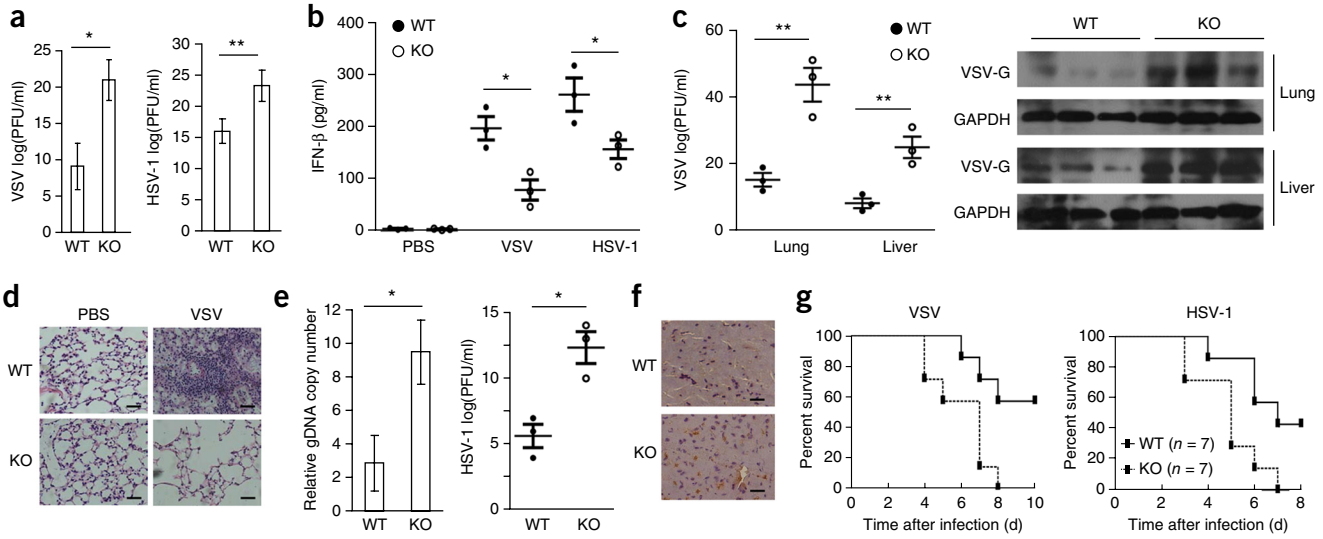

Figure 7 RNF128 positively regulates antiviral response. (**a**) VSV and HSV-1 titers in peritoneal macrophages from wild-type (WT) and *Rnf128*$^{-/-}$ (KO) mice infected with VSV (multiplicity of infection (MOI) 0.1) or HSV-1 (MOI 10). PFU, plaque-forming units. (**b**) IFN-β production in sera from KO and WT mice 8 h after intravenous injection with VSV or HSV-1 ($n = 3$ mice per group). (**c**) Plaque assay of VSV titers and immunoblot analysis of VSV-G protein in lung and liver from KO and WT mice ($n = 3$ mice per group) infected with the VSV for 72 h. (**d**) Hematoxylin–eosin staining of lung sections from KO and WT mice infected with VSV for 72 h. Scale bars, 40 μm. (**e**) HSV-1 genomic DNA copy number and viral titers in brain of KO and WT mice ($n = 3$ mice per group) infected with HSV-1 for 72 h. (**f**) ICP8-specific immunohistochemistry in the brains of HSV-1-infected mice ($n = 3$ mice per group). Scale bars, 40 μm. (**g**) Survival of KO and WT mice ($n = 7$ mice per group) after intravenous injection of VSV (4×10^7 PFU/mouse) or HSV-1 (2×10^7 PFU/mouse). $^*P < 0.05$, $^{**}P < 0.01$ (two-tailed Student's *t*-test (**a**–**c**,**e**) or Gehan–Breslow–Wilcoxon test (**g**)). Data are from 3 independent experiments (**a**–**c**,**e**; mean ± s.d. of triplicate assays) or are representative of 3 independent experiments with similar results (**c**,**d**,**f**).

did not induce IFN-β production or TBK1 phosphorylation when transfected into *Tbk1*$^{-/-}$MEFs (**Supplementary Fig. 5c**). We used Myc-TBK1-S172A to investigate whether RNF128 targets phosphorylated or unphosphorylated TBK1. We found that the extent of binding with RNF128 was similar between TBK1-S172A and TBK1-WT, as assessed by coimmunoprecipitation in HEK293 cells transfected with V5-RNF128-WT and Myc-TBK1-WT or Myc-TBK1-S172A (**Fig. 5d**). Furthermore, ubiquitination of TBK1-S172A induced by ectopic expression of V5-RNF128-WT was not lower than that of TBK1-WT in HEK293 cells (**Fig. 5e**), suggesting that RNF128-mediated TBK1 ubiquitination occurs upstream of TBK1 phosphorylation. Together, these data indicate that RNF128 promotes K63-linked ubiquitination of TBK1, leading to TBK1 phosphorylation and activation.

RNF128 is a general regulator for TBK1 activation

MIB1, MIB2 and Nrdp1 have been reported to promote K63-linked ubiquitination and activation of TBK1 (refs. 10,11). To evaluate the function of MIB1, MIB2 and Nrdp1 in relation to RNF128 on TBK1 activation, we designed three siRNAs for each and transfected them into *Rnf128*$^{-/-}$ peritoneal macrophages. MIB1 siRNA1 and siRNA2, MIB2 siRNA2 and Nrdp1 siRNA2 and siRNA3 efficiently attenuated the expression of their target genes and were used for subsequent experiments (**Fig. 6a**). LPS-, SeV- and HSV-1-induced *Ifnb1* expression and IRF3 and TBK1 phosphorylation were lower in *Rnf128*$^{-/-}$ peritoneal macrophages than in wild-type macrophages (**Fig. 6b**) and were further attenuated in SeV-infected, but not LPS-stimulated or HSV-1-infected, *Rnf128*$^{-/-}$ macrophages in which MIB1 and MIB2 were knocked down by siRNA (**Fig. 6b**). siRNA-mediated knockdown of Nrdp1 further decreased LPS-induced, but not SeV- or HSV-1-induced, *Ifnb1* expression, IRF3 and TBK1 phosphorylation in *Rnf128*$^{-/-}$ peritoneal macrophages (**Fig. 6b**). Simultaneous siRNA-mediated knockdown of MIB1, MIB2 and Nrdp1 in *Rnf128*$^{-/-}$ peritoneal macrophages decreased LPS- and SeV-induced, but not HSV-1-induced, *Ifnb1* expression and IRF3 and TBK1 phosphorylation (**Fig. 6b**). These data suggest that Nrdp1 has a role mainly in TBK1 activation downstream of LPS signaling, whereas MIB1 and MIB2 modulate TBK1 ubiquitination and activation upon RNA-virus infection, which is consistent with the reported roles of MIB1, MIB2 and Nrdp1 in the regulation of TBK1 ubiquitination[10,11]. Taken together, these results demonstrate that RNF128 is a general regulator for TBK1 ubiquitination and *Ifnb1* expression downstream of LPS-, RNA-virus- or DNA-virus-induced innate signaling.

RNF128 positively regulates antiviral responses

Type I interferons have critical roles in the immune response to viral infection[33]. Plaque assays showed that overexpression of V5-RNF128-WT in HEK293 cells infected with VSV substantially inhibited viral replication, as compared to empty (control) vector (**Supplementary Fig. 6a**). In contrast, overexpression of V5-RNF128-H2N2 or V5-RNF128-ΔPA did not inhibit viral replication (**Supplementary Fig. 6a**). Immunoblot analysis of VSV glycoprotein (VSV-G) expression indicated that VSV replication was significantly ($P < 0.05$) lower in HEK293 cells transfected with V5-RNF128-WT than in cells transfected with the control vector, but this was not the case with V5-RNF128-H2N2 or V5-RNF128-ΔPA (**Supplementary Fig. 6a**).

Plaque assays showed that transfection of mRNF128 increased VSV (**Supplementary Fig. 6b**) and HSV-1 (**Supplementary Fig. 6c**) replication in peritoneal macrophages, as compared to transfection with a 'scramble' siRNA (control). Similarly, siRNA-mediated knockdown of hRNF128 increased VSV (**Supplementary Fig. 6d**) and HSV-1 (**Supplementary Fig. 6e**) replication in THP-1 cells. VSV and HSV-1 replication were higher in in *Rnf128*$^{-/-}$ primary peritoneal macrophages than in wild-type macrophages (**Fig. 7a**).

To test the function of RNF128 *in vivo*, we challenged *Rnf128*$^{-/-}$ and wild-type mice with VSV and HSV-1. IFN-β protein abundance after

VSV or HSV-1 infection was much lower in the sera of *Rnf128*$^{-/-}$ mice (**Fig. 7b**). VSV titers and replication in the lung and liver were significantly higher in *Rnf128*$^{-/-}$ mice than in wild-type mice (**Fig. 7c**), and severe injuries were observed in the lungs of *Rnf128*$^{-/-}$ mice after infection with VSV (**Fig. 7d**). Similarly, copy numbers of HSV-1 genomic DNA and viral titers were significantly higher in the brains of *Rnf128*$^{-/-}$ mice than in their wild-type counterparts (**Fig. 7e**). Immunohistochemistry with antibody specific to the HSV-1 protein ICP8 indicated that *Rnf128*$^{-/-}$ mice had more HSV-1 virions in the brain than wild-type mice (**Fig. 7f**). *Rnf128*$^{-/-}$ mice showed higher mortality than wild-type mice upon infection with VSV or HSV-1 (**Fig. 7g**). These *in vivo* data indicate that RNF128 is an important positive regulator for antiviral immune responses against both RNA and DNA viruses.

DISCCUSION

Here, we demonstrated that the ubiquitin E3 ligase RNF128 interacts with TBK1 and promotes K63-linked ubiquitination of TBK1 after RNA- or DNA-virus infection. Our results in *Rnf128*$^{-/-}$ mice showed that RNF128 deficiency impairs RNA- and DNA-virus-induced IRF3 phosphorylation, IFN-β production and K63-linked ubiquitination and activation of TBK1. RNF128 interacted with TBK1 through the PA domain and mediated the K63-linked ubiquitination of TBK1 through the RING finger domain. The RNF128 mutants RNF128-H2N2 and RNF128-ΔPA, which have a nonfunctional RING domain and lack the PA domain, respectively, did not induce IFN-β production, IRF3 phosphorylation or TBK1 ubiquitination in HEK293 cells, leading to an inability to inhibit virus replication. LPS-induced IFN-β signaling was also impaired in RNF128-deficient cells. Therefore, RNF128 is a general regulator of K63-linked ubiquitination of TBK1 downstream of DNA-virus infection, RNA-virus infection and LPS stimulation.

Previously, two E3 ubiquitin ligases were found to promote K63-linked ubiquitination of TBK1. Deficiency or siRNA-mediated knockdown of MIB1 and MIB2 in MEFs or bone-marrow-derived macrophages (BMDMs) have been found to impair SeV-induced expression of *Ifnb1*, *Cxcl10* and *Ccl5* mRNA[10]. However, MIB1 and MIB2 do not regulate LPS- or DNA-virus-induced expression of *Ifnb1*, *Cxcl10* or *Ccl5* mRNA, suggesting that MIB1 and MIB2 specifically regulate TBK1 activation by double-stranded RNA or RNA-virus infection[10]. The E3 ubiquitin ligase Nrdp1 has also been shown to promote K63-linked ubiquitination of TBK1 (ref. 11). Knockdown of Nrdp1 expression in BMDMs impairs LPS-induced expression of *Ifnb1* and *Cxcl10* mRNA, indicating that Nrdp1 may be specifically involved in the regulation of LPS-induced TBK1 activation[11]. Here we confirmed the specificity of MIB1, MIB2 and Nrdp1 in relation to RNF128 on the regulation of TBK1 activation with siRNA-mediated knockdown experiments.

RNF128 is an important gatekeeper of T cell unresponsiveness[16]. Most previous studies of RNF128 have focused on CD4$^+$ T cells and adaptive immunity[17,18,34]. Here we provide evidence that RNF128 has an essential role in the regulation of innate antiviral response. RNF128 expression was induced upon infection with RNA virus or DNA virus; RNF128 increased IRF3 activation and IFN-β signaling upon infection with RNA virus or DNA virus; RNF128 deficiency or knockdown attenuated antiviral response both *in vitro* and *in vivo*, and RNF128 overexpression inhibited virus replication. Thus, our study defines RNF128 as a positive regulator of innate antiviral immunity in addition to its well-studied function in the regulation of T cells.

RNF128 controls T cells anergy and tolerance through K48-linked ubiquitination and degradation of several molecules involved in T cell activation. RNF128 interacts with and degrades T cell antigen receptor (TCR)–CD3 (ref. 18), CD40L[28], CD83 (ref. 29) and CD151 (ref. 27) through K48-linked ubiquitination. Here we showed that RNF128 promotes K63-linked ubiquitination of TBK1, identified a new substrate and delineated a new form of ubiquitination mediated by RNF128. Therefore, RNF128 may mediate both K48- and K63-linked ubiquitination leading to the degradation or activation of target proteins.

In summary, we have identified a RING-type E3 ligase that regulates TBK1 activation after both RNA-virus and DNA-virus infection. Given the pathological role of IFN-β in systemic lupus erythematosus and other autoimmune diseases, our data might provide some therapeutic clues for drug design to prevent excessive inflammation and limit viral infection.

METHODS

Methods and any associated references are available in the online version of the paper.

Note: Any Supplementary Information and Source Data files are available in the online version of the paper.

ACKNOWLEDGMENTS

We thank G.C. Fathman (Stanford University School of Medicine), K.A. Fitzgerald (University of Massachusetts Medical School) and H.-b. Shu (Wuhan University) for providing RNF128 expression plasmids, IFN-β reporter and TBK1 mutant plasmid S172A, respectively. We thank B. Sun (Institut Pasteur of Shanghai, Chinese Academy of Sciences) for providing TBK1-deficient MEFs, and H. Meng (Institute of Basic Medicine, Shandong Academy of Medical Sciences) for VSV and HSV-1. This work was supported in part by grants from the Natural Science Foundation of China (81525012, 81471538, 81273219) and the Specialized Research Fund for the Doctoral Program of Higher Education of China (20130131130010) to C.G. G.J. is a Taishan Scholar of Shandong, China.

AUTHOR CONTRIBUTIONS

C.G. conceived and supervised the study. G.S. performed most of the experiments and prepared the figures. B.L. performed part of the ubiquitination experiments. H.W., P.W., K.Z. and L.Z. provided reagents and contributed to discussions. Z.L. and G.J. provided facility for virus study. G.S. and C.G. analyzed the data and wrote the paper.

COMPETING FINANCIAL INTERESTS

The authors declare no competing financial interests.

1. Takeuchi, O. & Akira, S. Pattern recognition receptors and inflammation. *Cell* **140**, 805–820 (2010).
2. Alexopoulou, L., Holt, A.C., Medzhitov, R. & Flavell, R.A. Recognition of double-stranded RNA and activation of NF-κB by Toll-like receptor 3. *Nature* **413**, 732–738 (2001).
3. Yoneyama, M. *et al.* The RNA helicase RIG-I has an essential function in double-stranded RNA-induced innate antiviral responses. *Nat. Immunol.* **5**, 730–737 (2004).
4. Hornung, V. *et al.* 5′-triphosphate RNA is the ligand for RIG-I. *Science* **314**, 994–997 (2006).
5. Pichlmair, A. *et al.* RIG-I-mediated antiviral responses to single-stranded RNA bearing 5′-phosphates. *Science* **314**, 997–1001 (2006).
6. Kato, H. *et al.* Differential roles of MDA5 and RIG-I helicases in the recognition of RNA viruses. *Nature* **441**, 101–105 (2006).
7. Sun, L., Wu, J., Du, F., Chen, X. & Chen, Z.J. Cyclic GMP-AMP synthase is a cytosolic DNA sensor that activates the type I interferon pathway. *Science* **339**, 786–791 (2013).
8. Wu, J. & Chen, Z.J. Innate immune sensing and signaling of cytosolic nucleic acids. *Annu. Rev. Immunol.* **32**, 461–488 (2014).
9. Takeuchi, O. & Akira, S. Innate immunity to virus infection. *Immunol. Rev.* **227**, 75–86 (2009).
10. Li, S., Wang, L., Berman, M., Kong, Y.Y. & Dorf, M.E. Mapping a dynamic innate immunity protein interaction network regulating type I interferon production. *Immunity* **35**, 426–440 (2011).

11. Wang, C. *et al.* The E3 ubiquitin ligase Nrdp1 'preferentially' promotes TLR-mediated production of type I interferon. *Nat. Immunol.* **10**, 744–752 (2009).
12. Cui, J. *et al.* NLRP4 negatively regulates type I interferon signaling by targeting the kinase TBK1 for degradation via the ubiquitin ligase DTX4. *Nat. Immunol.* **13**, 387–395 (2012).
13. Zhang, M. *et al.* TRAF-interacting protein (TRIP) negatively regulates IFN-β production and antiviral response by promoting proteasomal degradation of TANK-binding kinase 1. *J. Exp. Med.* **209**, 1703–1711 (2012).
14. Friedman, C.S. *et al.* The tumour suppressor CYLD is a negative regulator of RIG-I-mediated antiviral response. *EMBO Rep.* **9**, 930–936 (2008).
15. Zhang, L., Zhao, X., Zhang, M., Zhao, W. & Gao, C. Ubiquitin-specific protease 2b negatively regulates IFN-β production and antiviral activity by targeting TANK-binding kinase 1. *J. Immunol.* **193**, 2230–2237 (2014).
16. Anandasabapathy, N. *et al.* GRAIL: an E3 ubiquitin ligase that inhibits cytokine gene transcription is expressed in anergic CD4+ T cells. *Immunity* **18**, 535–547 (2003).
17. Kriegel, M.A., Rathinam, C. & Flavell, R.A. E3 ubiquitin ligase GRAIL controls primary T cell activation and oral tolerance. *Proc. Natl. Acad. Sci. USA* **106**, 16770–16775 (2009).
18. Nurieva, R.I. *et al.* The E3 ubiquitin ligase GRAIL regulates T cell tolerance and regulatory T cell function by mediating T cell receptor-CD3 degradation. *Immunity* **32**, 670–680 (2010).
19. Bachmaier, K. *et al.* E3 ubiquitin ligase Cblb regulates the acute inflammatory response underlying lung injury. *Nat. Med.* **13**, 920–926 (2007).
20. Fang, D. & Liu, Y.C. Proteolysis-independent regulation of PI3K by Cbl-b-mediated ubiquitination in T cells. *Nat. Immunol.* **2**, 870–875 (2001).
21. Heissmeyer, V. *et al.* Calcineurin imposes T cell unresponsiveness through targeted proteolysis of signaling proteins. *Nat. Immunol.* **5**, 255–265 (2004).
22. Stetson, D.B. & Medzhitov, R. Recognition of cytosolic DNA activates an IRF3-dependent innate immune response. *Immunity* **24**, 93–103 (2006).
23. Darnell, J.E. Jr., Kerr, I.M. & Stark, G.R. Jak-STAT pathways and transcriptional activation in response to IFNs and other extracellular signaling proteins. *Science* **264**, 1415–1421 (1994).
24. Panne, D., Maniatis, T. & Harrison, S.C. An atomic model of the interferon-β enhanceosome. *Cell* **129**, 1111–1123 (2007).
25. Lin, R., Heylbroeck, C., Pitha, P.M. & Hiscott, J. Virus-dependent phosphorylation of the IRF-3 transcription factor regulates nuclear translocation, transactivation potential, and proteasome-mediated degradation. *Mol. Cell. Biol.* **18**, 2986–2996 (1998).
26. Yoneyama, M. *et al.* Direct triggering of the type I interferon system by virus infection: activation of a transcription factor complex containing IRF-3 and CBP/p300. *EMBO J.* **17**, 1087–1095 (1998).
27. Lineberry, N., Su, L., Soares, L. & Fathman, C.G. The single subunit transmembrane E3 ligase gene related to anergy in lymphocytes (GRAIL) captures and then ubiquitinates transmembrane proteins across the cell membrane. *J. Biol. Chem.* **283**, 28497–28505 (2008).
28. Lineberry, N.B. *et al.* Cutting edge: The transmembrane E3 ligase GRAIL ubiquitinates the costimulatory molecule CD40 ligand during the induction of T cell anergy. *J. Immunol.* **181**, 1622–1626 (2008).
29. Su, L.L., Iwai, H., Lin, J.T. & Fathman, C.G. The transmembrane E3 ligase GRAIL ubiquitinates and degrades CD83 on CD4 T cells. *J. Immunol.* **183**, 438–444 (2009).
30. Tu, D. *et al.* Structure and ubiquitination-dependent activation of TANK-binding kinase 1. *Cell Rep.* **3**, 747–758 (2013).
31. Larabi, A. *et al.* Crystal structure and mechanism of activation of TANK-binding kinase 1. *Cell Rep.* **3**, 734–746 (2013).
32. Kishore, N. *et al.* IKK-i and TBK-1 are enzymatically distinct from the homologous enzyme IKK-2: comparative analysis of recombinant human IKK-i, TBK-1, and IKK-2. *J. Biol. Chem.* **277**, 13840–13847 (2002).
33. van Boxel-Dezaire, A.H., Rani, M.R. & Stark, G.R. Complex modulation of cell type-specific signaling in response to type I interferons. *Immunity* **25**, 361–372 (2006).
34. Sahoo, A., Alekseev, A., Obertas, L. & Nurieva, R. Grail controls Th2 cell development by targeting STAT6 for degradation. *Nat. Commun.* **5**, 4732 (2014).

ONLINE METHODS

Mice. *Rnf128*$^{-/-}$ mice were from Jackson Laboratory. Genotyping of wild-type (WT) and knockout mice was performed with the following primers: forward primer 5′-CCAAAATCGATTCTCGTGGCTCC-3′ and reverse primer 5′-GGGCAAGTCCTGTGTTCTAAAAGC-3′ for WT mice; forward primer 5′-GCTGAAGTTAGTACTGCATG-3′ and reverse primer 5′-GTCAACAGG TGGCAGATACC-3′ for *Rnf128*$^{-/-}$ mice. All the mice were on the C57BL/6 background and were maintained under specific pathogen-free conditions with the approval of the Scientific Investigation Board of the Medical School of Shandong University.

Cells and reagents. HEK293, THP-1 and Vero cells were obtained from American Type Culture Collection. TBK1-deficient MEFs were provided by B. Sun. Mouse primary peritoneal macrophages were prepared from female C57BL/6J mice (5–6 weeks old) through intraperitoneal injection with thioglycolate. The cells were cultured at 37 °C under 5% CO_2 in DMEM supplemented with 10% FCS, 100 U/ml penicillin and 100 μg/ml streptomycin. ISD, poly(I:C) and phorbol ester (PMA) were purchased from InvivoGen. ISD and poly(I:C) were used at a final concentration of 10 μg/ml. Mouse recombinant IFN-β was from PeproTech and used at a final concentration of 1,000 U/ml. Sendai virus was purchased from China Center for Type Culture Collection. Vesicular stomatitis virus (VSV) and herpes simplex virus-1 (HSV-1) were provided by H. Meng. Information about the antibodies used in this study is provided in **Supplementary Table 1**.

Sequences, plasmids and transfection. Mutant expression plasmids for TBK1 (TBK1-K30R, TBK1-K401R and TBK1-K30R-K401R) were generated using the KOD-Plus-Mutagenesis kit (Toyobo). All constructs were confirmed by DNA sequencing. V5-RNF128-WT, V5-RNF128-H2N2 and V5-RNF128-ΔPA expression plasmids were provided by G.C. Fathman. The IFN-β, PRDI-III, PRDII and PRDIV reporter plasmids were provided by K.A. Fitzgerald. The TBK1 mutant plasmid TBK1-S172A was provided by H.-b. Shu. Other plasmids used in this study were described previously[35]. For transient transfection of plasmids and duplexes of siRNA into HEK293 cells, Lipofectamine 2000 was used (Invitrogen). For macrophages and THP-1 cells, plasmids and duplexes of siRNA were transfected into cells with the Geneporter 2 Transfection Reagent (Genlantis) according to the manufacturer's protocol. The sequences of siRNAs are listed in **Supplementary Table 2**. siRNAs were obtained from Genepharma except STAT1 siRNA and STAT2 siRNA, which were obtained from Santa Cruz Biotechnology.

ELISA. The concentrations of IFN-β in culture supernatants and sera were measured by ELISA Kits (R&D Systems).

RNA quantification. Total RNA was extracted with TRIzol reagent according to the manufacturer's instructions (Invitrogen). Primers used for RT-PCR assays are listed in **Supplementary Table 3**. Reverse-transcription products of samples were amplified by ABI 7300 Detection System (Applied Biosystems) using the SYBR Green PCR Master Mix (Toyobo) according to the manufacturer's instructions, and data were normalized by the level of GAPDH expression in each individual sample. The $2^{-\Delta\Delta Ct}$ method was used to calculate relative expression changes.

Assay of luciferase activity. Luciferase activity was measured with the Dual-Luciferase Reporter Assay system according to the manufacturer's instructions (Promega). Data were normalized for transfection efficiency by division of firefly luciferase activity by that of Renilla luciferase.

Coimmunoprecipitation and immunoblot analysis. For immunoblot analysis, cells or tissues were lysed with M-PER Protein Extraction Reagent (Pierce) supplemented with a protease inhibitor 'cocktail'. Protein concentrations in the extracts were measured with a bicinchoninic acid assay (Pierce) and were made equal with extraction reagent. For immunoprecipitation (IP), whole-cell extracts were collected 36 h after transfection and were lysed in IP buffer containing 1.0% (vol/vol) Nonidet P-40; 50 mM Tris-HCl, pH 7.4; 50 mM EDTA; 150 mM NaCl; and a protease inhibitor cocktail (Merck). After centrifugation for 10 min at 14,000 × *g*, supernatants were collected and incubated with protein G Plus-Agarose Immunoprecipitation reagent together with 1 μg corresponding antibodies. After 6 h of incubation, beads were washed five times with IP buffer. Immunoprecipitates were eluted by boiling with 1% (wt/vol) SDS sample buffer. For immunoblot analysis, immunoprecipitates or whole-cell lysates were loaded and subjected to SDS–PAGE, transferred onto nitrocellulose membranes and then blotted with indicated antibodies (**Supplementary Table 1**).

Ubiquitination assays. For analysis of the ubiquitination of TBK1 in HEK293 cells, cells were transfected with Myc-TBK1, HA-ubiquitin-WT or HA-ubiquitin mutants and V5-RNF128-WT or mutants, then whole-cell extracts were immunoprecipitated with anti-Myc and analyzed by immunoblot with anti-HA. For analysis of the ubiquitination of TBK1 in macrophages, macrophages were infected with SeV or HSV-1, then whole-cell extracts were immunoprecipitated with anti-TBK1 and analyzed by immunoblot with anti-ubiquitin.

***In vitro* binding and ubiquitination assay.** RNF128 and TBK1 proteins were expressed with a TNT Quick Coupled Transcription/Translation System (Promega). *In vitro* interaction and ubiquitination assays were performed as described[35].

TBK1 kinase assay. TBK1 kinase activity was assayed with ADP-Glo and TBK1 Kinase Enzyme System from Promega according to the instructions from the manufacturer. Briefly, TBK1 protein in the total cell extract was immunoprecipitated with anti-TBK1 antibody plus protein G beads by gentle rocking for 2 h at 4 °C followed by centrifugation for 5 min at 4 °C. Pellets were washed with lysis buffer (20 mM Tris-HCl, pH 7.4; 150 mM NaCl; 1 mM EDTA; 1% vol/vol Triton X-100; 2.5 mM sodium pyrophosphate; 1 mM β-glycerophosphate; 1 mM Na_3VO_4; and 1 mM phenylmethylsulfonyl fluoride). Each washed pellet was resuspended for 30 min at 30 °C in kinase assay buffer. TBK1 kinase activity was assayed with ADP-Glo and TBK1 Kinase Enzyme System.

Native PAGE. The IRF3 dimerization assay was performed as described[36]. In brief, macrophages were harvested with 50 μl ice-cold lysis buffer (50 mM Tris-HCl, pH 7.5; 150 mM NaCl; and 0.5% NP-40 containing protease inhibitor cocktail). After centrifugation at 13,000 × *g* for 10 min, supernatant protein was quantified and diluted with 2× native PAGE sample buffer (125 mM Tris-HCl, pH 6.8; 30% glycerol; and 0.1% bromophenol blue), and then 30 μg total protein was applied to a pre-run 7.5% native gel for separation. After electrophoresis, proteins were transferred onto a nitrocellulose membrane for immunoblotting.

Viral infection and plaque assay. HEK293, THP-1 or mouse primary peritoneal macrophages (2×10^5) were plated 24 h before infection. Cells were infected with VSV (0.1 MOI), SeV (1 MOI), or HSV-1 (10 MOI). VSV plaque assay and VSV replication were performed as described[35]. HSV-1 plaque assay was conducted in Vero cells. HSV-1 genomic DNA copy numbers were determined by real-time PCR using an HSV-1-specific primer: 5′-TGGGACACATGCCTTCTTGG-3′, 5′-ACCCTTAGTCAGACTCTGTT ACTTACCC-3′.

Virus infection *in vivo*. For *in vivo* virus infection studies, age- and sex-matched WT and *Rnf128*$^{-/-}$ littermate mice were intraperitoneally infected with VSV (4×10^7 PFU/mouse) or HSV-1 (2×10^7 PFU/mouse). Cytokine production in the sera was measured by ELISA. VSV titers in the lung and liver and HSV-1 titers in the brain were determined by standard plaque assays. For the survival experiments, mice were monitored for survival after VSV or HSV-1 infection. Lungs or brains from control- or virus-infected mice were dissected, fixed in 10% phosphate-buffered formalin, embedded into paraffin, sectioned, stained with hematoxylin–eosin solution and examined by light microscopy for histological changes.

Immunofluorescence staining and microscopy. HEK293 cells and macrophages cultured on cover slips were fixed for 10 min with 4% PFA and permeabilized for 20 min at room temperature with 0.5% Triton X-100. After incubation for blockade of nonspecific binding for 30 min, primary antibodies

were added and incubated for 2 h at room temperature. Samples were further stained with suitable Alexa Fluor 568– or Alexa Fluor 488–conjugated secondary antibodies (Thermo Fisher Scientific). Images were acquired on an Olympus IX71 fluorescence microscope (Olympus).

Statistical analysis. All data are presented as mean ± s.d. of 3 or more experiments. Statistical significance was determined with two-tailed Student's *t*-test, with $P < 0.05$ considered statistically significant. For mouse survival studies, Kaplan–Meier survival curves were generated and analyzed with GraphPad Prism 5.0. Pilot studies were used for estimation of sample size to ensure adequate power. No data points or mice were excluded from the study. No randomization or blinding was used.

35. Wang, P., Zhao, W., Zhao, K., Zhang, L. & Gao, C. TRIM26 negatively regulates interferon-β production and antiviral response through polyubiquitination and degradation of nuclear IRF3. *PLoS Pathog.* **11**, e1004726 (2015).
36. Mori, M. *et al.* Identification of Ser-386 of interferon regulatory factor 3 as critical target for inducible phosphorylation that determines activation. *J. Biol. Chem.* **279**, 9698–9702 (2004).

doi:10.1038/ni.3588